Hindawi Publishing Corporation
EURASIP Journal on Wireless Communications and Networking
Volume 2008, Article ID 865393, 11 pages
doi:10.1155/2008/865393

Research Article

An Evaluation of Interference Mitigation Schemes for HAPS Systems

Bon-Jun Ku,[1] Do-Seob Ahn,[1] and Nam Kim[2]

[1] *Department of Global Area Wireless Technology Research, Electronics and Telecommunications Research Institute, Daejeon 305-350, South Korea*
[2] *Information and Communication Engineering Division, Chungbuk National University, Cheongju 360-763, South Korea*

Correspondence should be addressed to Bon-Jun Ku, bjkoo@etri.re.kr

Received 28 September 2007; Revised 25 February 2008; Accepted 23 May 2008

Recommended by Abbas Mohammed

The International Telecommunication Union-Radiocommunication sector (ITU-R) has conducted frequency sharing studies between fixed services (FSs) using a high altitude platform station (HAPS) and fixed-satellite services (FSSs). In particular, ITU-R has investigated the power limitations related to HAPS user terminals (HUTs) to facilitate frequency sharing with space station receivers. To reduce the level of interference from the HUTs that can harm a geostationary earth orbit (GEO) satellite receiver in a space station, previous studies have taken two approaches: frequency sharing using a separated distance (FSSD) and frequency sharing using power control (FSPC). In this paper, various performance evaluation results of interference mitigation schemes are presented. The results include performance evaluations using a new interference mitigation approach as well as conventional approaches. An adaptive beamforming scheme (ABS) is introduced as a new scheme for efficient frequency sharing, and the interference mitigation effect on the ABS is examined considering pointing mismatch errors. The results confirm that the application of ABS enables frequency sharing between two systems with a smaller power reduction of HUTs in a cocoverage area compared to this reduction when conventional schemes are utilized. In addition, the analysis results provide the proper amount of modification at the transmitting power level of the HUT required for the suitable frequency sharing.

1. INTRODUCTION

A high-altitude platform station (HAPS) is a station that is located at an altitude of 20–50 km It is designed to provide various services in a wide coverage range over a terrestrial area and a short delay over a satellite network [1, 2]. Due to these service characteristics, HAPS is considered to be a new infrastructure that can substitute or fill in conventional systems, including terrestrial and/or satellite systems. Specifically, the possibility of utilizing HAPS as base stations for IMT-2000 services, as gateway links, and as an infrastructure for broadband wireless services has been investigated [3–5]. As HAPS utilizes the frequency bands previously allocated for conventional systems, investigations of issues on the frequency sharing between these systems have been conducted [6].

The International Telecommunication Union-Radiocommunication sector (ITU-R) has studied frequency sharing between HAPS and terrestrial systems for the IMT-2000 service, between HAPS and terrestrial systems for fixed services (FS), and between HAPS for FS and satellite systems for fixed-satellite services (FSSs) [7–9]. Due to the recent increase in the demand for broadband services, frequency sharing studies related to higher-frequency bands are very important for the efficient use of frequency resources. For this reason, ITU-R has conducted the studies related to limiting the transmit power of HAPS user terminals (HUTs) in order to protect satellite receivers utilizing the frequency bands of 47-48 GHz [10]. The 47-48 GHz frequency bands were previously allocated to the FFS spectrum to accommodate feeder links that serve to supply broadcasting satellite services [11].

As a part of these ITU-R study results, frequency sharing using a separated distance (FSSD) and frequency sharing using power control (FSPC) have been proposed [9, 12]. FSSD has been proposed for sharing between the HUTs of an HAPS system and a space station receiver of an FSS system [9]. The results show that the two systems cannot share the

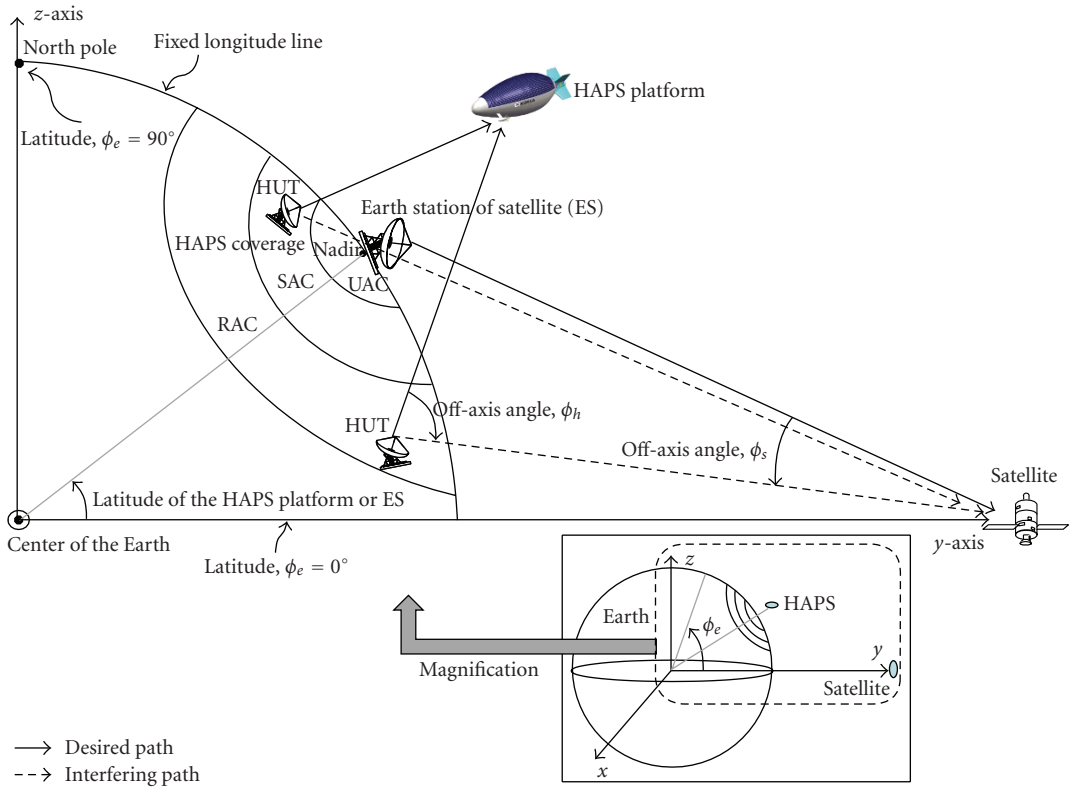

Figure 1: Description of HAPS and GEO systems.

same frequency band within a cocoverage area. The aggregate interference from the HUTs to a space station receiver would be minimally acceptable when there is no overlap between service areas. The use of FSSD is a simple approach that avoids harmful interference from HUTs to geostationary earth orbit (GEO) receivers in the space station. This is not desirable in terms of sharing because a very long separation distance may be required.

On the other hand, a recent study [12] demonstrated frequency sharing between two systems by applying an FSPC to the HUTs. Various methodologies have been investigated to determine the power level for the HUT; the results of these studies contributed to ITU-R. In this paper, several important points during the application of these two schemes for frequency sharing are addressed using the contribution results of [12] to ITU-R. Detailed performance evaluation results of these schemes are provided.

In addition to the aforementioned evaluations of conventional schemes, new evaluation results of frequency sharing studies applicable to the HUTs are introduced. Adaptive beamforming schemes (ABSs) are practically mandatory for future wireless communication systems, not only for efficient interference mitigation but also for high-quality service. However, there have been no reported results related to sharing via ABS between the two systems in the frequency bands of 47-48 GHz. ABS is applied to HUTs to maintain the main beam in the direction of the HAPS platform and to create a null condition in the direction of a GEO receiver. The performance of ABS is compared with that of FSPC by obtaining the cumulative distribution function (CDF) of the interference level. However, ABS is sensitive to errors caused by imprecise sensor calibrations. Considering this, the effects of the errors due to the pointing mismatch under the null condition are analyzed. Finally, a hybrid approach combining FSPC and ABS is applied in order to take advantage of both schemes and the performance evaluation results are presented.

This paper is organized as follows. Section 2 describes the system model and the related system parameters to calculate the interference level from the HUTs to a GEO receiver. Section 3 presents the methodology that calculates the interference from the HUTs to a GEO receiver. The procedure of calculating the CDF of the interference level that is received from the transmitted power of HUTs is then presented, and the estimation results are shown according to the latitude of the HAPS platform. After showing the interference analysis results using various conventional interference mitigation schemes including FSSD and FSPC in Section 4, new results are introduced using ABS and its variant in Section 5. This paper concludes with Section 6.

2. SYSTEM MODEL

2.1. System configuration

In this section, the system model that estimates the interference level from the HUTs to the satellite receiver is introduced [12]. Figure 1 shows the system model represented

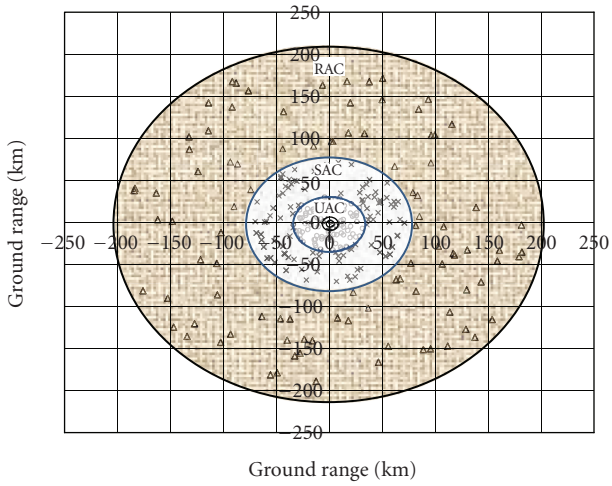

Figure 2: An example of HUT distribution.

Table 1: HAPS coverage zones.

Coverage area	Elevation angles (degrees)	Ground range (km)
UAC	90–30	0–36
SAC	30–15	36–76.5
RAC	15–5	76.5–203

in three-dimensional (3D) coordinates. At the bottom of Figure 1, a 3D constellation of an HAPS system exists along with a satellite in the GEO. Here, the target range was magnified to estimate the interference, and it is represented in the yz plane. The y- and z-axes represent the lines from the center of the Earth to the satellite and to the North Pole, respectively.

The HAPS system consists of the HAPS platform and a number of HUTs distributed in the HAPS coverage. The HAPS service coverage areas consist of urban area coverage (UAC), suburban area coverage (SAC), and rural area coverage (RAC) areas that are delineated mainly according to the elevation angles. This is based on the assumption that the HAPS nadir is located at the center of the UAC. SAC and RAC surround the UAC, as indicated in Figure 1.

The satellite system has a GEO receiver in a space station and an earth station (ES) based on the ground. As a satellite system is considered in the GEO, it is assumed that the HAPS platform is located at the same longitude with the satellite in a worst-case scenario. The satellite is located at the GEO, that is, $\phi_e = 0$ degrees, at a height that is 36,000 km above sea level. The ES of the satellite is located at the nadir of the HAPS platform to consider the worst case. The desired paths shown here as solid lines indicate the signal paths from HUTs to the HAPS platform in the HAPS system and the signal path from the ES to the satellite receiver in the satellite system. The interfering paths represented here as dotted lines indicate the signal paths from the HUTs to the satellite receiver. The angle ϕ_h is the off-axis angle from the main beam of a transmitting HUT antenna to the satellite, and the angle ϕ_s is the off-axis angle from the main beam of the receiving satellite antenna to a HUT.

2.2. HAPS system

HAPS service coverage zones are divided into UAC. SAC and RAC depending on the elevation angle of the HUTs, as shown in Table 1 [13]. Each coverage area has a maximum of 100 HUTs respectively. Each HUT has a bandwidth B of 2 MHz; the transmitting power density P_t and the maximum antenna gain $G_{\max}$ of the HUTs differ depending on the coverage area, as shown in Table 2 [13]. By analyzing the link budget of the HAPS system, it is possible to obtain the appropriate transmit power and antenna gain for the HUTs. It is assumed that the HUTs are distributed randomly in each zone. Figure 2 shows an example of a HUT distribution scheme on the ground.

The antenna beam pattern of [14] is used here for the HUT. The antenna beam pattern, $G_h(\phi_h)$ is expressed by

$$G_h(\phi_h) = \begin{cases} G_{\max} - 2.5 \times 10^{-3} \left(\dfrac{D}{\lambda}\phi_h\right)^2, & 0^\circ < \phi_h < \phi_m, \\ 2 + 15 \log \dfrac{D}{\lambda}, & \phi_m \le \phi_h < \dfrac{100\lambda}{D}, \\ 52 - 10 \log \dfrac{D}{\lambda} - 25 \log \phi_h, & \dfrac{100\lambda}{D} \le \phi_h < 48^\circ, \\ 10 - 10 \log \dfrac{D}{\lambda}, & 48^\circ \le \phi_h \le 180^\circ, \end{cases} \tag{1}$$

where $G_{\max}$ and D are the maximum antenna gain defined in Table 2 and the antenna diameter of the HUT, respectively, and λ is the wavelength in meters. ϕ_m is given by

$$\phi_m = \frac{20\lambda}{D} \sqrt{G_{\max} - 2 + 15 \log \frac{D}{\lambda}}. \tag{2}$$

Figure 3 shows the relative amplitude response with the off-axis angle, ϕ_h, of the transmitting HUT antenna using (1).

2.3. GEO satellite system

A GEO satellite system consists of a GEO receiver in a space station and an ES on the ground. An interference criterion of -150.5 dB (W/MHz) is used for the satellite system defined

Table 2: HUT transmitter parameters.

Coverage area (Total number of terminals)	Power density, P_t, (dB(W/MHz))	Maximum antenna gain, $G_{\max}$, (dBi)	Bandwidth, B, (MHz)
UAC (100)	−8.2	23	2
SAC (100)	−7	38	2
RAC (100)	−1.5	38	2

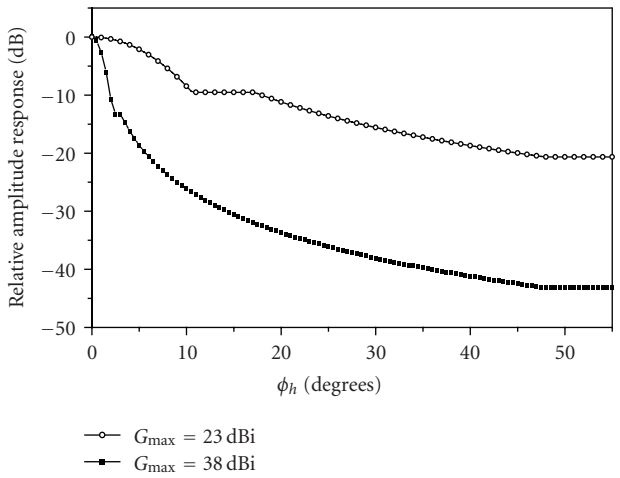

Figure 3: Antenna beam patterns for the HUT.

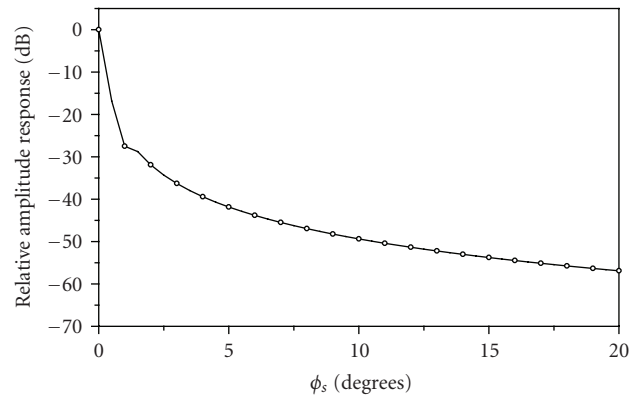

Figure 4: Antenna beam pattern for the GEO receiver.

in [9]. For the GEO receiver, antenna beam pattern of [15], $G_s(\phi_s)$, is used, as expressed by

$$G_s(\phi_s) = \begin{cases} G_{\max} - 3\left(\dfrac{\phi_s}{\phi_{3\,\mathrm{dB}}}\right)^2, & \phi_{3\,\mathrm{dB}} \le \phi_s \le 2.58\phi_{3\,\mathrm{dB}}, \\ G_{\max} - 25, & 2.58\phi_{3\,\mathrm{dB}} < \phi_s \le 6.32\phi_{3\,\mathrm{dB}}, \\ G_{\max} - 25 + 25\log\phi_s, & 6.32\phi_{3\,\mathrm{dB}} < \phi_s \le 6.32\phi_{3\,\mathrm{dB}} \\ & \times 10^{0.04(G_{\max}-25)}, \\ 0, & 6.32\phi_{3\,\mathrm{dB}}10^{0.04(G_{\max}-25)} \\ & < \phi_s \le 90^\circ, \\ -10 + 0.25G_{\max}, & 90^\circ < \phi_s \le 180^\circ. \end{cases} \tag{3}$$

Here, the maximum antenna gain, $G_{\max}$ for the satellite receiver is 51.8 dBi and one-half the 3 dB beamwidth, $\phi_{3\,\mathrm{dB}}$, is given by [15]

$$\phi_{3\,\mathrm{dB}} \approx 10^{(44.5-G_{\max})/20}. \tag{4}$$

Figure 4 shows the antenna beam pattern using the off-axis angle ϕ_s of a satellite receiver. To compare the coverage of the satellite with that of HAPS, the diameter of the coverage, l_c is calculated in km using

$$l_c = \frac{2 \times 36,000}{\tan(90^\circ - \phi_{3\,\mathrm{dB}})}. \tag{5}$$

The service coverage of a satellite on the ground is approximately 271 km in diameter at the equator. The coverage includes all of the HUTs in UAC and SAC as well as most of them in RAC, implying that the GEO receiver may experience strong interference from the HUTs.

3. ESTIMATION OF THE INTERFERENCE LEVEL

In this section, the methodology that calculates the interference level from the HUTs to the GEO receiver is presented. Figure 5 shows the geometric configuration for the estimation of the interference between the HAPS and satellite systems. Referring to the 3D coordinate configuration in Figure 1, the coordinates of the ith HUT, HUT^i, are denoted as (x_i, y_i, z_i). Similarly, the coordinates of the HAPS platform, the GEO receiver, and the ES are $(0, y_h, z_h)$, $(0, h_s, 0)$, and $(0, y_e, z_e)$, respectively. The angle ϕ_h^i represents the off-axis angle to the satellite from the main beam of the transmitting HUT^i antenna. The angle ϕ_s^i represents the off-axis angle from the main beam of the receiving satellite antenna to the HUT^i.

The estimated receiving interference power density received by the GEO receiver can be calculated as [9]

$$P_r = \sum_i \Big(P_t^i + G_h(\phi_h^i) + G_s(\phi_s^i) - L_a(\theta_i) - 10\log B - 20\log\frac{4\pi d}{\lambda} - 60 \Big), \ \mathrm{dB(W/MHz)}, \tag{6}$$

where P_t^i is the transmitting output power density from the ith HUT, $G_h(\phi_h^i)$ is the transmitting antenna gain for the

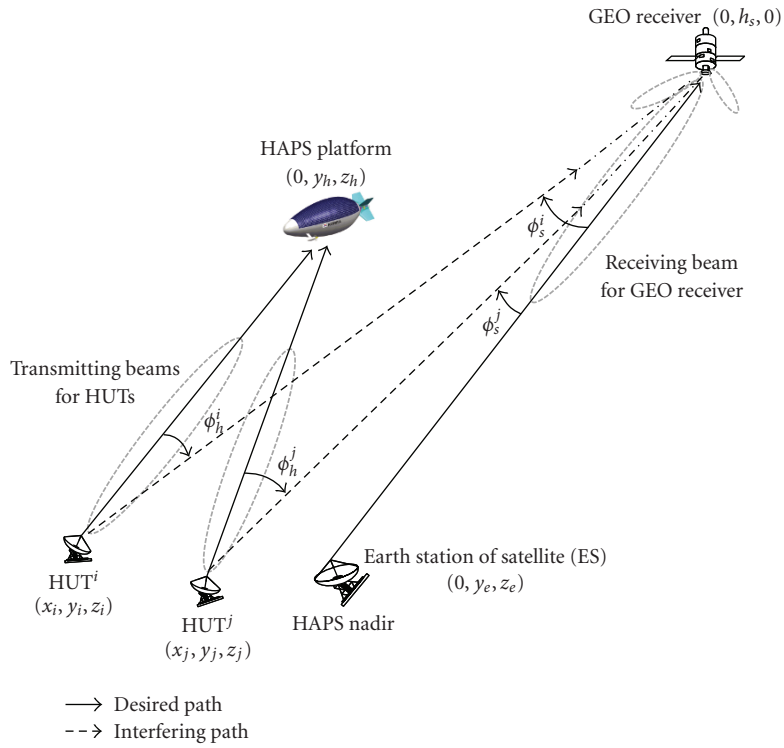

Figure 5: Geometric configuration for interference estimation.

off-axis angle ϕ_h^i of the ith HUT, $G_s(\phi_s^i)$ is the receiving antenna gain for the off-axis angle ϕ_s^i of the satellite antenna, $L_a(\theta_i)$ is atmospheric absorption for the elevation angle from θ_i the ith HUT, λ is the wavelength in meters, and d is the distance between the HUT and the satellite in km. Thus, P_r can be regarded as the aggregated interference power from all HUTs.

In order to estimate P_r in (6), 300 locations of HUTs were randomly generated. The antenna gain with the off-axis angles for the HUTs and the GEO receiver were initially obtained. The off-axis angles, ϕ_h^i and ϕ_s^i, can be calculated from

$$\phi_h^i = \cos^{-1}\left[\frac{(l_{h\_p}^i)^2 + (l_{h\_s}^i)^2 - (l_{p\_s}^i)^2}{2\cdot(l_{h\_p}^i)^2\cdot(l_{h\_s}^i)^2}\right],$$
$$\phi_s^i = \cos^{-1}\left[\frac{(l_{h\_s}^i)^2 + (l_{s\_e}^i)^2 - (l_{h\_e}^i)^2}{2\cdot(l_{h\_s}^i)^2\cdot(l_{s\_e})^2}\right], \tag{7}$$

where $l_{h\_p}^i$, $l_{h\_s}^i$, $l_{p\_s}^i$, l_{s_e}, and $l_{h\_e}^i$ represent the path lengths from HUT^i to the HAPS platform, from HUT^i to the GEO receiver, from the HAPS platform to the GEO receiver, from the GEO receiver to the ES, and from HUT^i to the ES, respectively. The path lengths can be obtained from the coordinates of the HUTs, the HAPS platform, the GEO receiver, and the ES.

Here, the propagation attenuation term $L_a(\theta_i)$ in (6) is considered. Assuming that the height of HUTs is zero, the atmosphere attenuation $L_a(\theta_i)$ is defined by (8) in the frequency band from 47.9 GHz to 48.2 GHz [8]. This depends on the elevation angle θ_i of the ith HUT and the latitude ϕ_e of the HAPS platform:

$$L_a(\theta_i) = \begin{cases} \dfrac{57.90}{1 + A_1\theta_i + A_2\theta_i^2 - A_3\theta_i^3 + A_4\theta_i^4}, & 0^\circ \le \phi_e < 22.5^\circ, \\ \dfrac{53.06}{1 + B_1\theta_i + B_2\theta_i^2 - B_3\theta_i^3 + B_4\theta_i^4}, & 22.5^\circ \le \phi_e < 45^\circ, \\ \dfrac{53.21}{1 + C_1\theta_i + C_2\theta_i^2 - C_3\theta_i^3 + C_4\theta_i^4}, & \phi_e \ge 45^\circ. \end{cases} \tag{8}$$

Here, the constants from A_1 to C_4 are given by Table 3.

One thousand independent simulations were run and the CDF of the interference levels was then estimated. Figure 6 shows the estimated CDF, that is, the cumulative probability of interference, I, that is less than or equal to I_0 in the x-abscissa. It was found that the interference level increases as the HAPS platform moves to a higher latitude, as the possibility that HUTs at higher latitudes can face directly toward a GEO receiver is high. For example, if the latitude of the HAPS platform is greater than 50 degrees, the probability of the aggregate interference to the GEO receiver exceeding the interference criterion is 100%. If the latitude of the HAPS platform is 30 degrees, the probability of the aggregate interference satisfying the criterion is only 10%. This implies that a proper interference mitigation scheme (IMS) is required.

Table 3: Constant values.

Constants	Values	Constants	Values	Constants	Values
A_1	0.7262	B_1	0.6962	C_1	0.6864
A_2	0.03534	B_2	0.03555	C_2	0.03632
A_3	0.001074	B_3	0.001076	C_3	0.001103
A_4	0.7826×10^{-5}	B_4	0.7840×10^{-5}	C_4	0.8073×10^{-5}

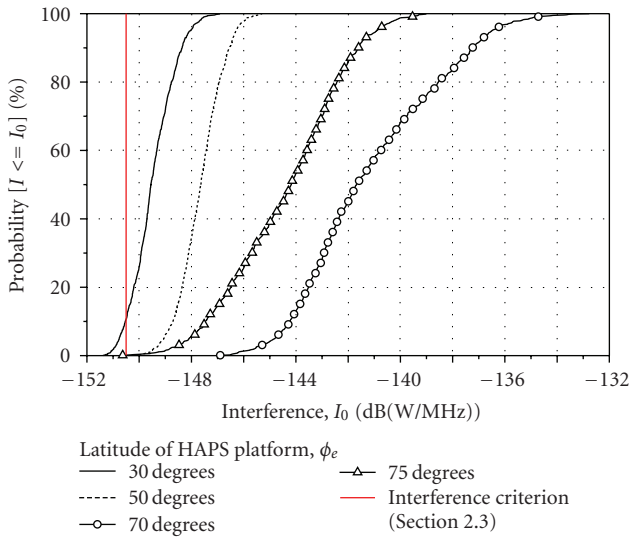

Figure 6: Interference level with the latitude of the HAPS platform ϕ_e.

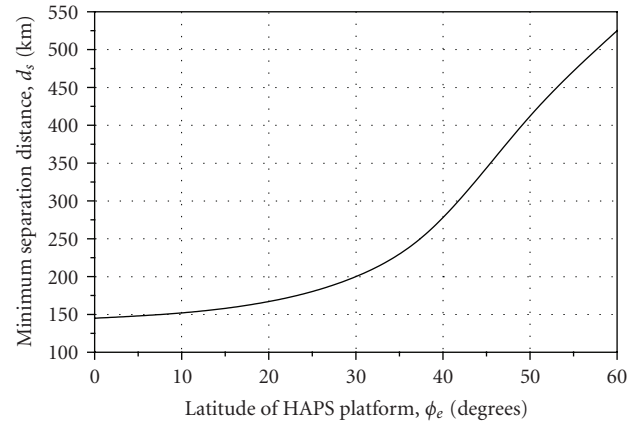

Figure 7: Separation distance with the latitude of the HAPS platform ϕ_e.

4. INTERFERENCE ANALYSIS USING CONVENTIONAL APPROACHES

4.1. FSSD approach

The separation distance can be considered as an easy means of determining the sharing condition between wireless systems. In a previous study by [9, 16], the separation distance satisfying the criterion of a GEO receiver was estimated. Figure 7 shows the minimum separation distance, d_s, required to satisfy the interference criterion according to various HAPS platform latitudes as represented by ϕ_e. If the HAPS platform is located at the latitudes $\phi_e = 0°$, the separation distance d_s should be more than 145 km between the HAPS nadir and the ES. As more HUTs face a GEO receiver as the latitude of the HAPS platform ϕ_e increases, a greater separation distance is needed at a higher latitude. FSSD is a simple but inefficient way to bring this about, as a very long separation distance may be required for two systems to use the same frequency bands.

4.2. FSPC approach

As an alternate approach to FSSD, FSPC can be used. In this section, the concept and results of a performance evaluation of the FSPC are given, and several problems when applying it are discussed using the contribution results to ITU-R originally proposed by [12].

HAPS using frequency bands of 47-48 GHz may experience significant rain attenuation; such a system requires a sufficient rain attenuation margin to overcome it. However, during most clear-sky days, these relatively high margins have been shown to result in harmful interference to a satellite system [9]. This implies that an appropriate power control mechanism can reduce the interference level. A methodology to determine the minimum required power level for the HUT using FSPC was investigated, and the results are presented in the Recommendation ITU-R SF.1843 [12]. The results show that perfect sharing can be achieved between HUTs and a GEO receiver in a cocoverage area, that is, without any distance separation.

In the FSPC scheme, the transmit power level of the HUT is controlled. This reduces the harmful interference in the direction of a GEO receiver. If HUTs are equipped with power control systems, they can reduce or increase the transmit power depending on the conditions and not exceed the interference criterion of the GEO receiver in a cocoverage area. In clear-sky conditions, HUTs reduce these power levels, and on rainy days, they increase the power up to the rain attenuation margin defined in [13].

Figure 8 shows the CDF of the interference levels for the FSPC scheme according to various latitudes of the HAPS platform ϕ_e. A power control range, P_R, of 5 dB as defined in [12] is used here; Figure 8 shows that the interference levels do not exceed the interference criterion

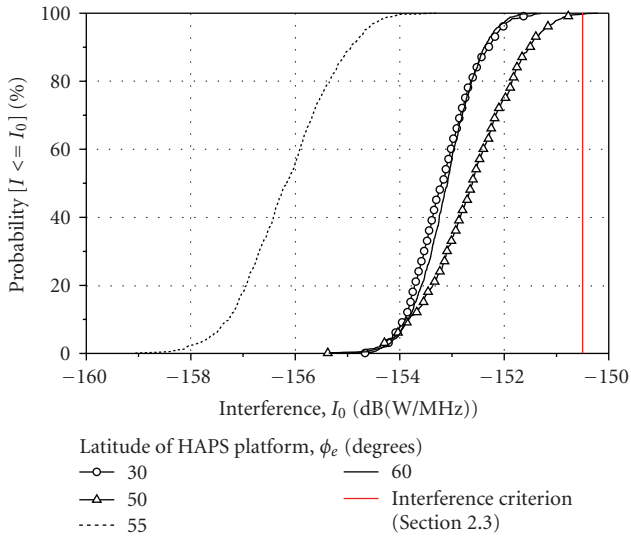

Figure 8: Interference level with the latitude of an HAPS platform ϕ_e, using the FSPC scheme (P_R = 5 dB).

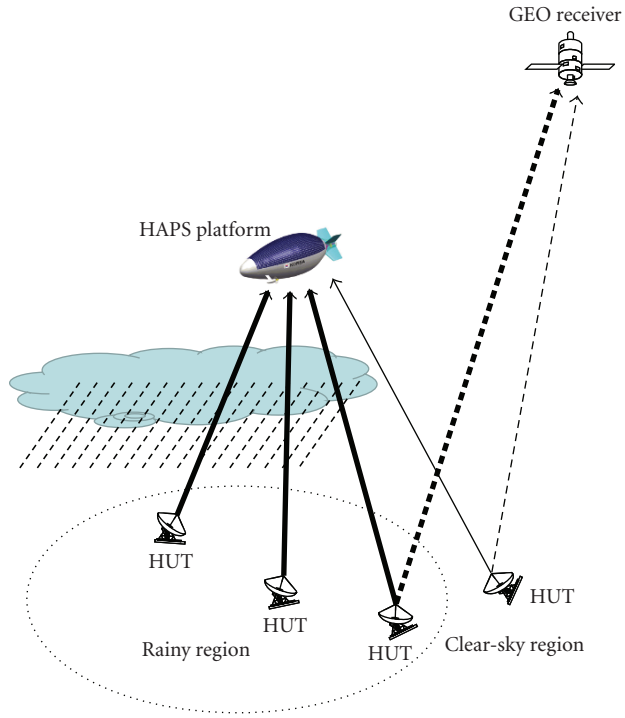

Figure 9: Scenario in the case of strong interference.

with any ϕ_e value. However, any HUTs power control failure may cause a power loss of up to 5 dB, which can lead to serious performance degradation of the HAPS system. In addition, as shown in Figure 9, if a HUT is located at a border of a rainy region and a clear-sky region, the signal path from the HUT to the satellite does not experience any rain attenuation, which may cause strong interference. For this reason, an efficient technique to control the antenna sidelobes is required, leading to an efficient beamforming technique. This is investigated in detail in the next section.

5. A NEW ANALYSIS RESULTS

5.1. Ideal ABS approach

5.1.1. Basic concept

Adaptive beamforming can provide an efficient means of interference mitigation. Figure 10 shows an example of a HUT system with an adaptive beamforming device. The system consists of receiving and transmitting beamformers. The number of elements, M, determines the antenna gain of the HUT. The incident wave impinges on the array at any angles that are normal to the array surface. The signal in each branch is weighted in order to point to the target. It is assumed that the same weighting vectors are used in the receiver and the transmitter, that is, $[w_0^{\text{in}}, w_1^{\text{in}}, \ldots, w_{M-1}^{\text{in}}] = [w_0^{\text{out}}, w_1^{\text{out}}, \ldots, w_{M-1}^{\text{out}}]$. This is discussed in Section 5.1.2.

It is assumed that the system is equipped with a minimum-variance beamformer (MVB) in [17] and that the HUT can estimate the optimum weighting vectors to reduce the interference signal in the direction of the GEO receiver. Here, the antenna beam pattern of the MVB for the interference analysis is presented. MVB is used to minimize the variance of the input signals with the interfered signals, satisfying the constraint in which the power for the desired direction should be characterized by unity. Assuming M linear array elements spaced by a half wavelength between them in the receiving module, this concept can be expressed as [18]

$$w = \underset{w^* a(\theta_e)=1}{\arg \min} w^* R_x w, \tag{9}$$

where w is the M-by-1 optimum weighting vector of the beamformer, R_x is the M-by-M correlation matrix of the received signal covariance, and $a(\theta_e)$ is the M-by-1 steering vector with the electrical angle θ_e related to the angle of incidence ϕ_h that is normal to the array surface defined by

$$\theta_e = \pi \sin \phi_h. \tag{10}$$

Here, T and $*$ represent the transposition of a matrix and complex conjugate of the matrix.

Generally, it is possible to solve the optimum solution given in (9) using the method of *Lagrange* [18, 19]. Combining the variance equation defined by $w^* R_x w$ with the constrained part $w^* a(\theta_e) = 1$ gives

$$w_{\text{mv}} = \frac{R_x^{-1} a(\theta_e)}{a(\theta_e)^* R_x^{-1} a(\theta_e)}. \tag{11}$$

The MVB with the optimal solution (11), having been designed to minimize $w^* R_x w$ in (9) while preserving the

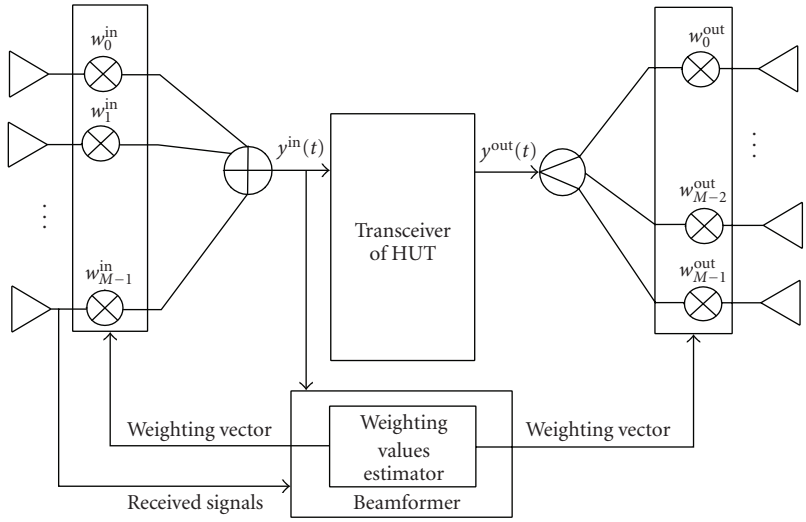

Figure 10: Block diagram for the HUT using ABS.

signal for the direction of the HAPS platform, imposes a null in the direction of GEO.

Via (11), the antenna beam pattern of the MVB can be expressed as

$$G(\phi_h) = 10\log_{10}\left|w_{\text{mv}}^H a(\theta_e)\right|^2. \tag{12}$$

5.1.2. Analysis on the frequency translation effect

In the previous section, it was assumed that the same weighting vectors are used in the receiver and the transmitter. Here, the effect of this is analyzed. The concept of the reuse of the weight has been introduced for land mobile cellular systems [20]. For the time-division duplex (TDD), the weight obtained during the receiving time slot can be reused in the transmitting time slot as a fixed parameter, as the carrier frequency of the uplink, f_u, is equal to that of the downlink, f_d. This no longer holds for the frequency-division duplex (FDD) [20, 21]. Generally, utilizing the same array weight gives rise to null positioning error between the up- and down-link, as the antenna element spacing normalized by the wavelength varies in proportion to the difference in frequency. A good example of this is a beamforming system with FDD in the IMT-2000 frequency bands that uses a carrier frequency of 2140 MHz for the downlink and 1950 MHz for the uplink. Figure 11 compares the beam patterns of the receiver and the transmitter when the interfering signal is at 25 degrees. If the same array weights are used for the receiver and the transmitter, a comparatively large null pointing error of approximately 2.5 degrees is produced. This is shown in Figure 11. To address this issue, Ohgane proposed the reconfiguration of the weight vector by comparing the transmitting and receiving array patterns and adjusting the weight value for transmission [20].

This is analyzed in the application of HAPS FDD system. According to Resolution 122 (Rev. WRC-2007), the frequency bands 47.9–48.2 GHz and 47.2–47.5 GHz, each

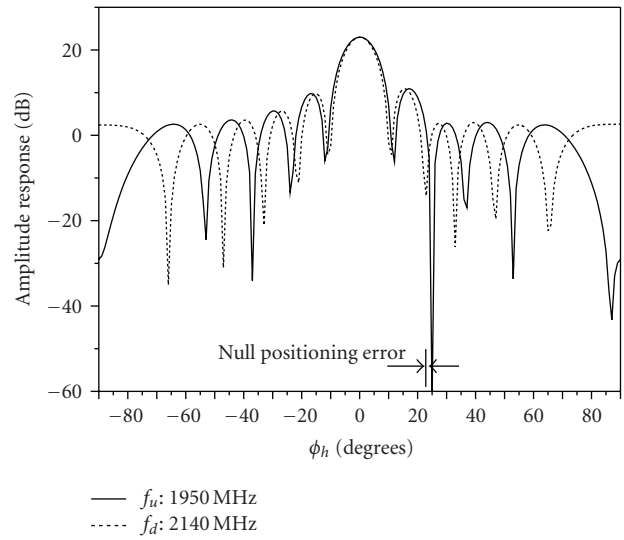

Figure 11: Comparison of the beam patterns of the receiver and transmitter using IMT-2000 frequency bands.

with 300 MHz bandwidth, can be used for the HAPS. Here, 48.05 GHz is used as the carrier frequency of the uplink, f_u, and 47.35 GHz is used as the carrier frequency of the downlink, f_d. The bandwidth of 300 MHz is very narrow in the target frequency bands, as the percentage of the bandwidth for the carrier frequency is only 0.62%. Figure 12 compares the beam patterns of the receiver and the transmitter when the interfering signal is at 25 degrees. As shown in the figure, the beam patterns are nearly identical for f_u and f_d, despite the fact that the same weights are used for the receiver and the transmitter. This implies that the same weighting factors can be used without any performance degradation.

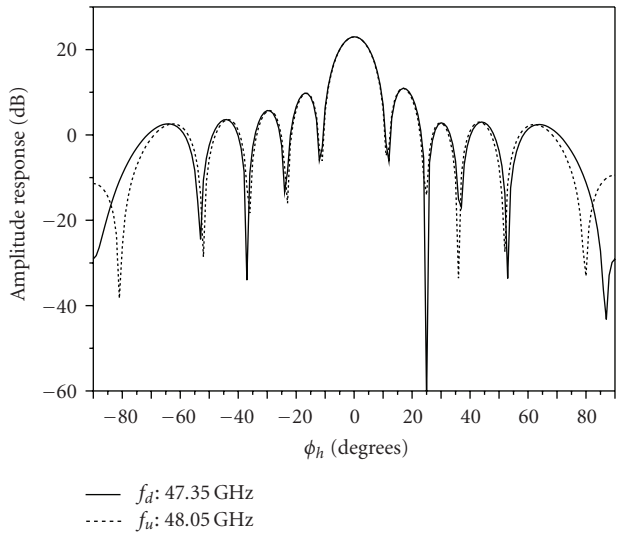

Figure 12: Comparison of the beam pattern of the receiver and the transmitter of the HUT using MVB.

5.1.3. Interference analysis results

An important factor related to the reduction of the interference that is harmful to the GEO receiver is that a very low sidelobe level of the HUTs that face the GEO receiver should be obtained. The same analysis procedure from (6) to (8) used in the previous section is followed using the antenna beam pattern in (12).

Figure 13 shows an example of the adaptive beam patterns when the $G_{\max}$ values of the HUT are 23 dBi and 38 dBi, respectively, (see Table 2). In this example, the desired and interfering direction is 0 and 30 degrees, respectively. When the antenna beam patterns in (12) are used for the transmitting beams, a symmetric beam for all direction can be assumed by extending the 2D antenna beam pattern in Figure 13 to 3D. As shown in Figure 14, when the ABS is applied to the HUTs, two systems can share a cocoverage without any power reduction in the HUTs.

5.2. Hybrid approach

The ABS can cause pointing errors at the null, which may introduce harmful interference to other systems. In order to offset this pointing error, the FSPC approach can be used in conjunction with the ABS. The effect of the error due to the null pointing mismatch on the amount of interference to the satellite is initially analyzed. It is assumed that M linear array elements with the uniform amplitude distribution experience pointing error at the null defined by [22]

$$\sigma_{\Delta}^2 = \frac{12}{M^3}\sigma_{\Phi}^2, \tag{13}$$

where σ_{Δ}^2 is the variance of the pointing error and σ_{Φ}^2 is the phase error variance. The parameters σ_{Φ} of contemporary microwave amplifiers can provide a phase nonidentity within a limit of 10 degrees [23]. In the case of phase distribution errors of 5 and 10 degrees, the total range of the pointing

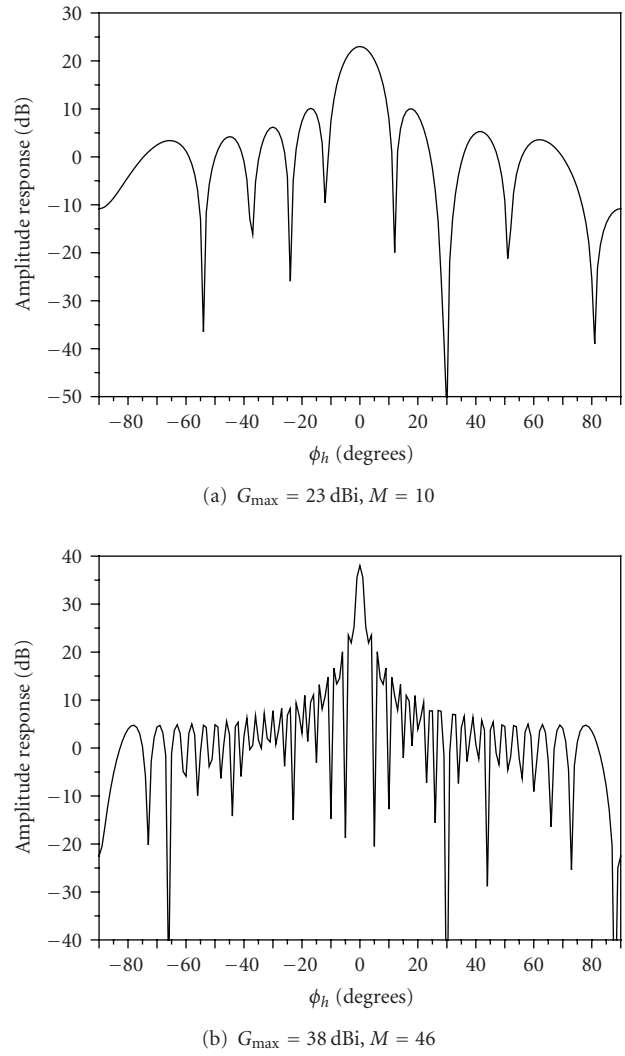

Figure 13: An example of an antenna beam pattern using ABS.

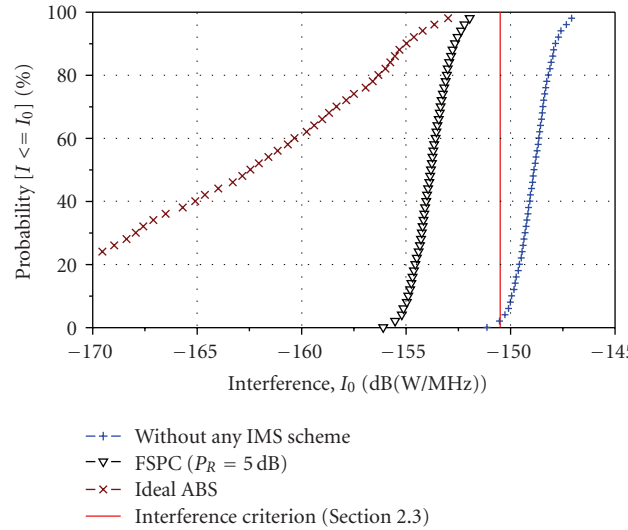

Figure 14: CDF of interference levels for ideal ABS and FSPC schemes.

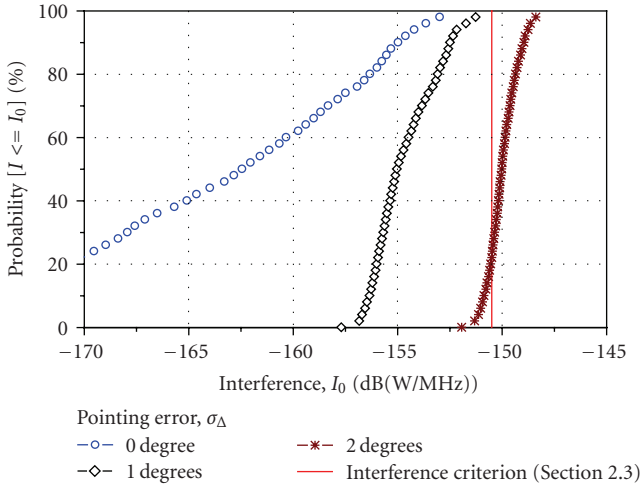

Figure 15: CDF of interference levels according to the pointing errors, σ_Δ.

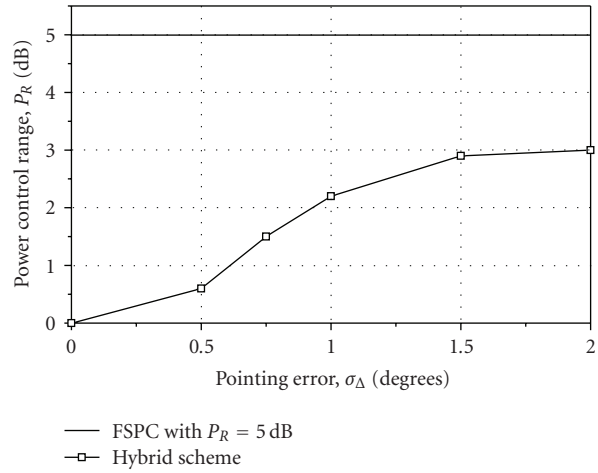

Figure 16: Power control range, P_R, according to the pointing errors, σ_Δ.

error is approximately 1 and 2 degrees, respectively. Figure 15 shows the CDF of the interference levels according to various pointing error values. If pointing errors are not controlled within at least 1 degree, the aggregated interference level may exceed this criterion. In order to overcome the increase in the interference due to the pointing error, a hybrid method that combines ABS with FSPC can be used. The advantage of the hybrid scheme can be understood by comparing the required power control range that regulates the interference to the satellite. A large power control range indicates a high probability of system outage in case of failure or error in power control scheme. Therefore, the outage probability can be reduced using the ABS with the reduced power control range. Figure 16 shows the required power control range according to the σ_Δ value of the ABS scheme compared to the conventional FSPC scheme. It is clear that, even with a very large value of σ_Δ, the power control range can be reduced considerably. For example, the reduction in the power control range exceeds 50% and 40% if the σ_Δ value is 1 and 2 degrees, respectively.

6. CONCLUSION

Sharing issues between FS using HAPS and FSS systems were studied with a focus on the uplink from HUTs to a GEO receiver. In this paper, several sharing methodologies based on the FSSD and FSPC were presented. The FSSD is a simple approach that avoids harmful interference from HUTs to a GEO receiver. However it is not desirable in terms of sharing. The FSPC also has a drawback in that reducing the power levels of the HUTs may result in performance degradation of the HAPS system.

In this paper, an interference mitigation effect was demonstrated by applying the ABS to HUTs in a manner that overcomes the aforementioned drawbacks. However, HUTs using ABS may give rise to interference that is harmful to a satellite receiver when an amount of beam pointing error exists due to phase disturbance on the array antenna elements. Finally, a hybrid approach combining FSPC with ABS considering the beam pointing errors was presented. From the analysis results, it was shown that the two systems can share the same frequency bands in a cocoverage case even when beam pointing errors pertaining to HUTs exist. The present analysis results reveal that an ABS scheme combined with FSPC can reduce the power control range by 40% compared to a conventional FSPC scheme.

ACKNOWLEDGMENTS

This work was supported by the IT R&D program of KCC/IITA[2008-F-013-01, Development of spectrum engineering and millimeterwave utilizing technology]. The authors wish to thank Professor Dr. Sooyoung Kim for useful discussions that significantly improved earlier versions of this paper.

REFERENCES

[1] T. C. Tozer and D. Grace, "High-altitude platforms for wireless communications," *Electronics & Communication Engineering Journal*, vol. 13, no. 3, pp. 127–137, 2001.

[2] Radio Regulations, Footnote 1.66A, International Telecommunication Union (ITU), 2004.

[3] D. Grace, J. Thornton, G. Chen, G. P. White, and T. C. Tozer, "Improving the system capacity of broadband services using multiple high-altitude platforms," *IEEE Transactions on Wireless Communications*, vol. 4, no. 2, pp. 700–709, 2005.

[4] B. Taha-Ahmed, M. Calvo-Ramon, and L. de Haro-Ariet, "High altitude platforms (HAPs) W-CDMA system over cities," in *Proceedings of the 61st IEEE Vehicular Technology Conference (VTC '05)*, vol. 4, pp. 2673–2677, Stockholm, Sweden, May-June 2005.

[5] G. P. White and Y. V. Zakharov, "Data communications to trains from high-altitude platforms," *IEEE Transactions on Vehicular Technology*, vol. 56, no. 4, pp. 2253–2266, 2007.

[6] Word Radiocommunication Conference Final Acts, ITU, 2003.

[7] Recommendation ITU-R M.1641, "A methodology for co-channel interference evaluation to determine separation distance from a system using high-altitude platform stations to a cellular system to provide IMT-2000 service within the boundary of an administration," ITU, 2006.

[8] Recommendation ITU-R F. 1501, "Coordination distance for systems in the fixed service (FS) involving high-altitude platform stations (HAPSs) sharing the frequency bands 47.2–47.5 GHz and 47.9–48.2 GHz with other systems in the fixed service," ITU, 2000.

[9] Recommendation ITU-R SF. 1481-1, "Frequency sharing between systems in the fixed service using high-altitude platform stations and satellite systems in the geostationary orbit in the fixed-satellite service in the bands 47.2–47.5 and 47.9–48.2 GHz," ITU, 2002.

[10] Resolution 122 (revised in World Radiocommunication Conference (WRC)—2003), "Use of the bands 47.2–47.5 GHz and 47.9–48.2 GHz by high altitude platform stations (HAPS) in the fixed service and by other services," ITU, 2003.

[11] Radio Regulations, Footnote 5.552A, International Telecommunication Union (ITU), 2004.

[12] Recommendation ITU-R SF. 1843, "Methodology for determining the power level for ground terminals to facilitate sharing with space station receivers in the bands 47.2–47.5 GHz and 47.9–48.2 GHz," ITU, 2007.

[13] Recommendation ITU-R F. 1500, "Preferred characteristics of systems in the fixed service using high altitude platforms operating in the bands 47.2–47.5 GHz and 47.9–48.2 GHz," ITU, 2000.

[14] Recommendation ITU-R F. 699, "Reference radiation patterns for fixed wireless system antennas for use in coordination studies and interference assessment in the frequency range from 100 MHz to about 70 GHz," ITU, 2003.

[15] Recommendation ITU-R S. 672, "Satellite antenna radiation pattern for use as a design objective in the fixed-satellite service employing geostationary satellites," ITU, 1997.

[16] B.-J. Ku, J.-M. Park, and D.-S. Ahn, "Analyzing separation distance from HAPS to satellite earth station in V band," in *Proceeding of the 21st International Technical Conference in Circuit/Systems, Computers and Communications (ITC-CSCC '06)*, vol. 2, pp. 441–444, Chiang Mai, Thailand, July 2006.

[17] J. Capon, "High-resolution frequency-wavenumber spectrum analysis," *Proceedings of IEEE*, vol. 57, no. 8, pp. 1408–1418, 1969.

[18] S. Haykin, *Adaptive Filter Theory*, Prentice Hall Information and System Sciences Series, Prentice Hall, Englewood Cliffs, NJ, USA, 1996.

[19] J. Litva, *Digital Beamforming in Wireless Communications*, Artech House, Boston, Mass, USA, 1996.

[20] T. Ohgane, "Spectral efficiency improvement by base station antenna pattern control for land mobile cellular systems," *IEICE Transactions on Communications*, vol. E77-B, no. 5, pp. 598–605, 1994.

[21] G. Xu and H. Liu, "Effective transmission beamforming scheme for frequency-division-duplex digital wireless communication systems," in *Proceedings of the 20th IEEE International Conference on Acoustics, Speech and Signal Processing (ICASSP '95)*, vol. 3, pp. 1729–1732, Detroit, Mich, USA, May 1995.

[22] R. J. Mailloux, *Phased Array Antenna Handbook*, Artech House, Boston, Mass, USA, 1994.

[23] B.-J. Ku, D.-S. Ahn, S.-P. Lee, et al., "Radiation pattern of multibeam array antenna with digital beamforming for stratospheric communication system: statistical simulation," *ETRI Journal*, vol. 24, no. 3, pp. 197–204, 2002.